



Sensitive infrared spectroscopy of isoprene at the part per billion level using a quantum cascade laser spectrometer

Jacob T. Stewart¹ · Jacob Beloin¹ · Melanie Fournier¹ · Grace Kovic¹

Received: 24 February 2020 / Accepted: 7 October 2020 / Published online: 17 October 2020
© Springer-Verlag GmbH Germany, part of Springer Nature 2020

Abstract

A quantum cascade laser-based infrared spectrometer equipped with a multipass cell has been used to perform sensitive infrared spectroscopy of isoprene at part per billion (ppbv) concentration levels. The instrument was used to measure the absorption of the strong Q-branch of the ν_{26} vibrational mode of isoprene near 992 cm^{-1} to determine isoprene concentrations in gas-phase samples. The response of the spectrometer is highly linear in the concentration range measured (0.3–10.5 parts per million by volume) and the lowest noise-equivalent concentration determined for the spectrometer is 3.2 ppbv at an optimal averaging time of 9 s when performing measurements at atmospheric pressure. At reduced pressure (190 Torr), the lowest noise-equivalent concentration increases to 9 ppbv, but the reduced pressure decreases spectral interference caused by absorption peaks from other chemical species, namely ammonia, methanol, and carbon dioxide. The spectrometer was used to directly measure the isoprene concentration in breath samples from a volunteer without any sample processing, showing the potential real-world application of the present approach.

1 Introduction

Trace gases play an important role in the chemistry of Earth's atmosphere, making it essential to develop methods to measure their concentrations. Isoprene (C_5H_8) is a trace gas that is the most abundant biogenic volatile organic compound (BVOC) emitted into Earth's atmosphere, comprising roughly 50% of total BVOC emissions globally [1, 2]. Isoprene is readily oxidized by ozone and hydroxyl radical, leading to a relatively short atmospheric lifetime, on the order of hours, and a low atmospheric concentration, on the order of a few parts per billion by volume (ppbv) [1]. Oxidation of isoprene has been shown to contribute to the formation of secondary organic aerosols [3], particularly in the presence of anthropogenic oxidants such as nitric oxides [4]. The oxidation of isoprene in the presence of nitric oxides also leads to the formation of tropospheric ozone, a harmful pollutant that is a major component of smog [5]. The ozone-forming potential of isoprene is particularly important in major urban centers, where there is a high flux of

anthropogenic nitric oxides, and prompted a recent study of isoprene emission in Beijing [6].

In addition to its importance in atmospheric chemistry, isoprene is also one of the most abundant hydrocarbons in human breath. Breath isoprene has been linked to the cholesterol biosynthesis pathway and there is interest in measuring isoprene as a way to perform noninvasive monitoring of patients [7]. For example, a 2015 study showed that breath isoprene can be used as a marker for advanced fibrosis in individuals with chronic liver disease [8] and a recent study from 2018 examined the possibility of measuring isoprene exhaled from audiences watching movies as an aid in film classification [9].

Several methods are currently used for measuring isoprene (and other volatile organic compounds) in atmospheric and breath samples, including gas chromatography with flame ionization (GC-FID) or mass spectrometric (GC-MS) detection, proton transfer reaction mass spectrometry (PTR-MS) [10, 11], and chemoresistive sensors made from metal oxide nanoparticles [12–14]. Gas chromatography and mass spectrometric methods provide good selectivity and high sensitivity, with detection limits in the parts per trillion (pptv) range, but the instrumentation is costly and has somewhat limited portability. Chemoresistive sensors are significantly more portable and affordable, but suffer from somewhat poor selectivity for isoprene

✉ Jacob T. Stewart
jstewar3@conncoll.edu

¹ Department of Chemistry, Connecticut College,
New London, CT 06320, USA

and decreased sensitivity, with detection limits in the parts per billion (ppbv) range. There has recently been a call for “simple, stable, and affordable” ways to measure BVOCs to provide continuous monitoring of molecules like isoprene on the ecosystem scale to better understand their emission dynamics [15]. Infrared laser spectroscopy is one possible tool to enable “simple, stable, and affordable” measurements of BVOCs, with the capability of rapid measurements at high sensitivity with moderate costs. Spectral databases such as HITRAN [16] and the PNNL spectral library [17] provide important data to enable quantitative infrared measurements. Infrared spectrometers, particularly those based on quantum cascade lasers (QCLs), have become popular for measuring trace gases in the atmosphere [18–20]. For example, QCL-based spectrometers have been employed for trace gas detection of ammonia [21, 22], methane [23, 24], and nitrous oxide [24, 25], among many other molecules [26]. QCL-based spectroscopy methods provide the advantage of rapid measurements that can be performed in situ rather than needing to collect air samples to analyze in a lab. As QCL technology has progressed over the last two and a half decades, the price of lasers has decreased and the performance of the lasers has increased, making QCL spectrometers more affordable and capable instruments.

Though infrared spectroscopy is routinely used to measure many atmospheric molecules, there have only been a few studies published in recent years using infrared spectroscopy to study isoprene. In 2002, Kühnemann et al. [27] reported an infrared photoacoustic spectrometer for measuring isoprene emission from plants. Their instrument used a sealed-off CO₂ laser as the light source targeting the strong isoprene absorption bands near 10 μm. They were able to achieve a detection limit of 400 pptv for isoprene (and 600 pptv for the doubly deuterated isotopomer) with this instrument and used it to measure isoprene emission from a *Eucalyptus globulus* tree. In 2010, Adler et al. [28] used a mid-IR frequency comb coupled to a multipass cell to measure isoprene, among several other molecules, achieving an experimental detection limit of 7 ppbv. More recently, in 2014 Brauer et al. [29] presented quantitative absorption cross sections for isoprene measured across the entire infrared spectrum using a Fourier transform spectrometer to support future efforts using infrared spectroscopy for quantifying isoprene in air samples. Another study published in 2014 by Perez-Guaita et al. [30] combined Fourier transform infrared spectroscopy in a substrate-integrated hollow waveguide with a preconcentration system to detect isoprene in human breath. The authors demonstrated a limit of detection of 32 ppbv for isoprene using this system and were able to detect isoprene in a breath sample from a volunteer.

In the current study, we present a direct absorption QCL spectrometer using a multipass cell which is capable of measuring concentrations of isoprene in the ppbv range.

We describe the layout of the spectrometer and then present measurements made with the spectrometer to assess its performance, including the measurement of isoprene in breath samples from a volunteer. We will also discuss future prospects for using infrared laser spectroscopy with QCLs for performing atmospheric or breath analysis measurements.

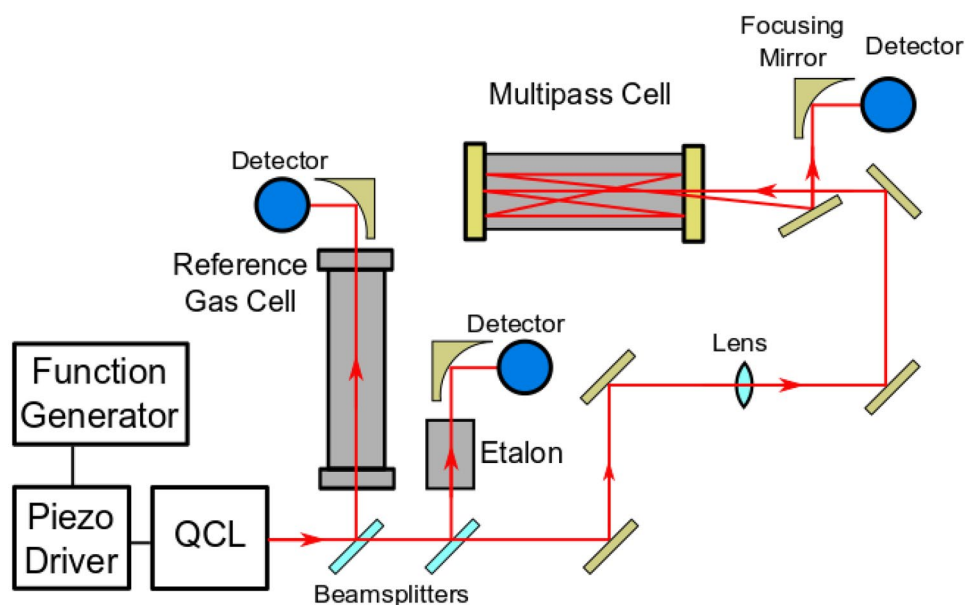
2 QCL-based spectrometer

The spectrometer used in this study is similar to the instrument previously used in our lab to study the high-resolution spectrum of isoprene in the region of the ν_{26} vibrational band (see Fig. 1) [31]. There have been some changes to the spectrometer which will be described below. The light source for the spectrometer is a mode hop free external cavity QCL from Daylight Solutions. This QCL has mode hop free tuning from 962–1019 cm⁻¹, which covers the ν_{26} vibrational band of isoprene. Light from the laser is sent through two beamsplitters, and one of the beams is directed through a reference gas cell containing a low pressure of methanol for absolute frequency calibration. After exiting the reference gas cell, the light is focused using an off-axis parabolic mirror onto a room temperature photovoltaic MCT detector (Vigo Systems, PVM-10.6-1×1). The second beam is directed through a germanium etalon with a free spectral range of 0.0245 cm⁻¹, which provides relative frequency calibration. The etalon was not present in the previous version of the spectrometer. After passing through the etalon, the light is focused using an off-axis parabolic mirror onto another room temperature photovoltaic MCT detector (Vigo Systems, PVM-10.6-1×1). The third and final beam is sent through a neutral density filter to decrease the laser power and focused into a multipass absorption cell (76 m pathlength, Aerodyne Research, AMAC-76) where isoprene samples are measured. The light exiting the multipass cell is focused with an off-axis parabolic mirror onto a thermoelectrically cooled MCT detector (Vigo Systems, PVI-2TE10.6-1×1).

In this study, the laser frequency was scanned using a piezoelectric transducer built into the external cavity of the QCL. The piezo was driven with a sine wave at a rate of 60 Hz using a piezo controller (ThorLabs, MDT694B) driven by a function generator. This is the maximum sweep rate that is recommended by Daylight Solutions for this laser model. To avoid possible asymmetries in the spectra between the up and down sweeps of the sine wave, only the downward sweeps were used for analysis. Each scan of the piezo is capable of covering approximately 0.7–0.8 cm⁻¹, which is sufficient to cover the main Q-branch peak of the ν_{26} band.

The data from the detectors are digitized using a data acquisition card (Measurement Computing, USB-1808X)

Fig. 1 Layout of the QCL-based spectrometer used in this study



which is capable of recording each channel simultaneously at a sampling rate of up to 200 kHz. This data acquisition card is one of the major changes in this version of the spectrometer, with a significantly higher sampling rate than our previous card, which was only capable of sampling the channels non-simultaneously at a rate of 4 kHz. Most spectra reported in this study were acquired at a sampling rate of 150 kHz, though some were recorded at a rate of 100 kHz. This allows us to sweep the piezo at the maximum rate of 60 Hz and still resolve the etalon and methanol features for frequency calibration. The acquired data were saved to a personal computer using a custom Python program. After acquisition, the spectra were calibrated using a combination of the etalon spectrum and the methanol spectrum. The relative frequency calibration was obtained from the spacing of the peaks in the etalon spectrum. The relative frequency axis was then adjusted for each spectrum by comparing the measured methanol spectrum to a reference methanol spectrum generated using the SpectraPlot website [32], which is based on the HITRAN database [16].

To test the capabilities of the spectrometer we used a certified 10.8 ± 0.5 ppmv mixture of isoprene in nitrogen (Airgas) which was further diluted using high-purity nitrogen (Airgas) to obtain lower concentrations. The dilution was performed by flowing the isoprene mixture and nitrogen into the multipass cell and monitoring the flow rate with a pair of mass flowmeters (Omega, Model FMA-A2304, accuracy of $\pm 1\%$). The flow from each gas was controlled using a needle valve and the overall pressure in the cell was maintained by manually adjusting a valve between the multipass cell and a vacuum pump. The pressure was monitored using a capacitance manometer (MKS Baratron, Model 626C13TBE, accuracy of 0.25%).

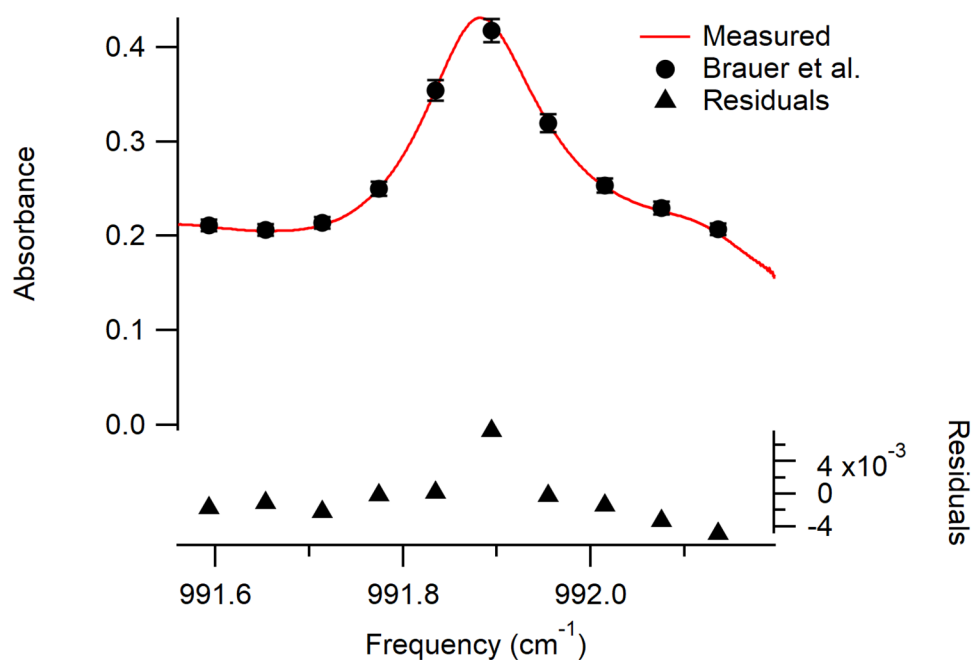
3 Spectrometer performance

3.1 Measurement of certified sample

As mentioned in the introduction, quantitative infrared spectra of isoprene at atmospheric pressure have previously been reported by Brauer et al. [29] We used their reported spectra, as obtained from the PNNL spectral library [17], to verify the accuracy of our spectrometer. Figure 2 shows a typical absorption spectrum of the certified isoprene sample recorded with our spectrometer at atmospheric pressure (760 Torr). The sample and background spectra were recorded for 1 s each, and represent the average of 60 individual frequency sweeps of the laser. For the background spectrum, the multipass cell was filled with high-purity nitrogen at atmospheric pressure. The averaged spectra were used to calculate the absorbance. Using the path length of 76 m for our multipass cell, we used the reported spectrum of Brauer et al. to retrieve the concentration of our certified sample. The retrieved concentration is 10.5 ppmv, within the certified concentration range of 10.3–11.3 ppmv provided by the supplier. Figure 2 shows a comparison between our measured spectrum and a simulated spectrum based on the data from Brauer et al. for a 10.5 ppmv sample measured over a pathlength of 76 m. Our data lie within the 3% error given by Brauer et al. (represented as error bars in the figure) for their absorbance values.

As can be seen in Fig. 2, our spectra are obtained at significantly higher frequency resolution than the data from Brauer et al. Because of this, we used the absorption spectrum shown in Fig. 2 for further concentration determinations in this study. To perform the determinations, the absorption spectrum in Fig. 2 was used as a reference

Fig. 2 Typical absorption spectrum of the certified 10.8 ± 0.5 ppmv mixture of isoprene in nitrogen (red line) compared to a simulated spectrum of isoprene at a concentration of 10.5 ppmv based on the measurements of Brauer et al. [29] (black dots). The error bars indicate the 3% error in absorption values given by Brauer et al. for their measurements. Residuals between the measured data and simulated data are shown below the figure (black triangles)



spectrum after being scaled to the expected absorption for a 1 ppmv sample in our 76 m pathlength cell. Measured absorption spectra were then fit to the following equation in the region of the strongest peak between 991.7 and 992.1 cm^{-1} to determine the isoprene concentration:

$$A_{\text{measured}}(\tilde{\nu}) = c_{\text{isoprene}} \times A_{\text{reference}}(\tilde{\nu}) \quad (1)$$

Here, A_{measured} is the measured absorbance spectrum as a function of wavenumber, c_{isoprene} is the concentration of isoprene in ppmv, and $A_{\text{reference}}$ is the reference absorption spectrum scaled to a 1 ppmv concentration.

3.2 Linearity of the instrument

To test the linearity of the spectrometer, seven different dilutions of the certified isoprene mixture were made with concentrations of 8.8, 5.9, 3.5, 1.9, 0.66, 0.65, and 0.34 ppmv. For each of these samples, ten spectra were acquired for 0.25 s each, and one background spectrum of nitrogen was acquired for each mixture. The resulting spectra were used to determine the absorbance of each sample, which was used to determine the concentration of isoprene using the process outlined in the previous section. The average concentration of the ten measurements was then determined. Part A of Fig. 3 shows a plot of the average measured concentration values using the spectrometer versus the concentration of each prepared sample. As can be seen, the instrument has highly linear behavior, with a slope of 1.000 ± 0.004 and a y-intercept of 0.03 ± 0.02 for the linear fit.

As a further comparison of the prepared and measured isoprene concentrations, part B of Fig. 3 presents a Bland–Altman plot showing the differences between the measured isoprene concentration and the nominal concentration of the mixtures as prepared using the flowmeters. The average difference is 0.03 ppmv with a standard deviation of 0.04 ppmv (depicted as horizontal lines on the plot). The average relative error for the measured values compared to the nominal values is $\sim 3\%$. The accuracy of our spectrometer, at least in comparison with the accuracy of our sample mixing, is in the tens of ppbv range. This is somewhat higher than our detection limit (about 3 ppbv, see next section) and is at least partially caused by a systematic difference in the two flowmeters that were used to measure the dilution of the samples. When the flowmeter used to measure the flow of high purity nitrogen was instead used to measure the flow of the isoprene standard and vice versa, the difference between the measured and prepared concentrations were consistently negative instead of positive.

3.3 Detection limit

The stability and detection limit of the instrument were examined by measuring an ~ 8 ppmv isoprene mixture for 30 min using the spectrometer. A background spectrum of nitrogen was acquired after the 30 min of measurements and was used to calculate the absorbance for each acquired spectrum. Each spectrum was measured for 0.5 s, which represents averaging about 30 sweeps of the laser over the isoprene Q-branch. Additional time was needed for saving the data and averaging the spectra in the software, which leads

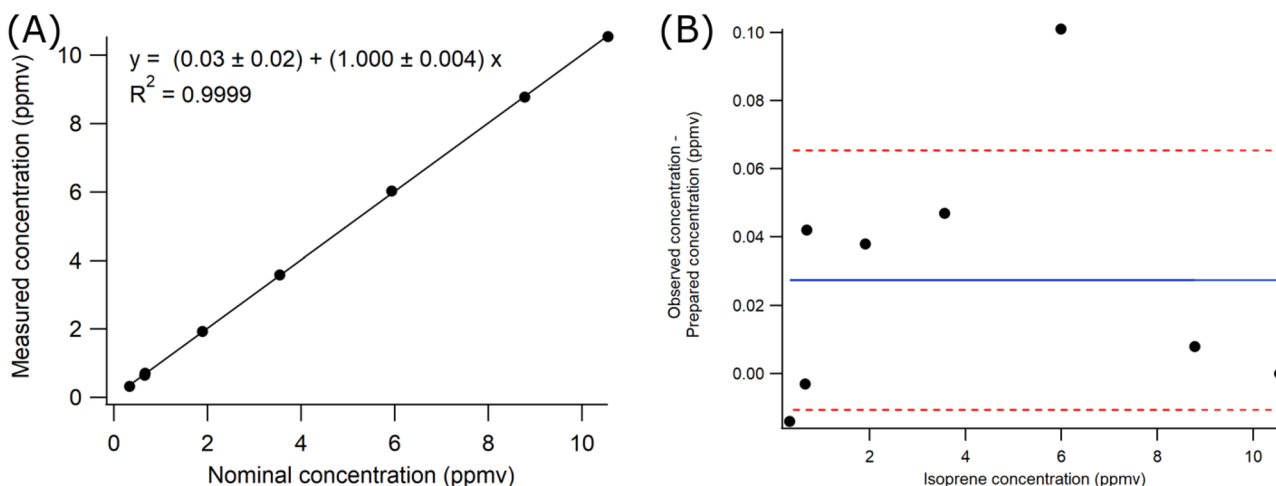


Fig. 3 **a** Comparison of measured isoprene concentrations using the QCL spectrometer and the prepared concentrations made by diluting a certified isoprene sample. The equation of the best-fit line is given on the plot and shows the linear behavior of the instrument. **b** Bland–Altman plot of the differences between the measured isoprene

concentrations compared to the prepared concentrations for the measurements shown in (a). The solid blue line indicates the average difference of 0.03 ppmv and the dashed red lines indicate the standard deviation of the differences (± 0.04 ppmv)

to a total measurement time of 1.25 s for each spectrum that was acquired. The retrieved concentrations are shown in part a of Fig. 4. The Allan deviation plot calculated from this dataset is shown in part b of Fig. 4. From the plot, it can be seen that the lowest noise-equivalent concentration for our instrument is 3.2 ppbv at an optimal averaging time of 9 s.

It is apparent from the measured concentrations and Allan deviation plot that our instrument suffers from drift which limits our ability to decrease the detection limit of the spectrometer by averaging for long periods of time. We are not completely certain what is causing this drift, but it has been

consistent over the course of months of using the spectrometer. One of the main sources of this drift appears to be inconsistent power output from the EC-QCL. We have observed that background spectra acquired with only nitrogen differ slightly when measured over the course of several minutes, which affects the absorbance values and lines up with the time scale of the drift observed in Fig. 4. The ultimate cause of this inconsistency may be temperature drift either in the EC-QCL or in our lab. Another possible source of noise in the system is mechanical vibrations affecting the multipass cell. We have attempted to reduce the effects of vibration by

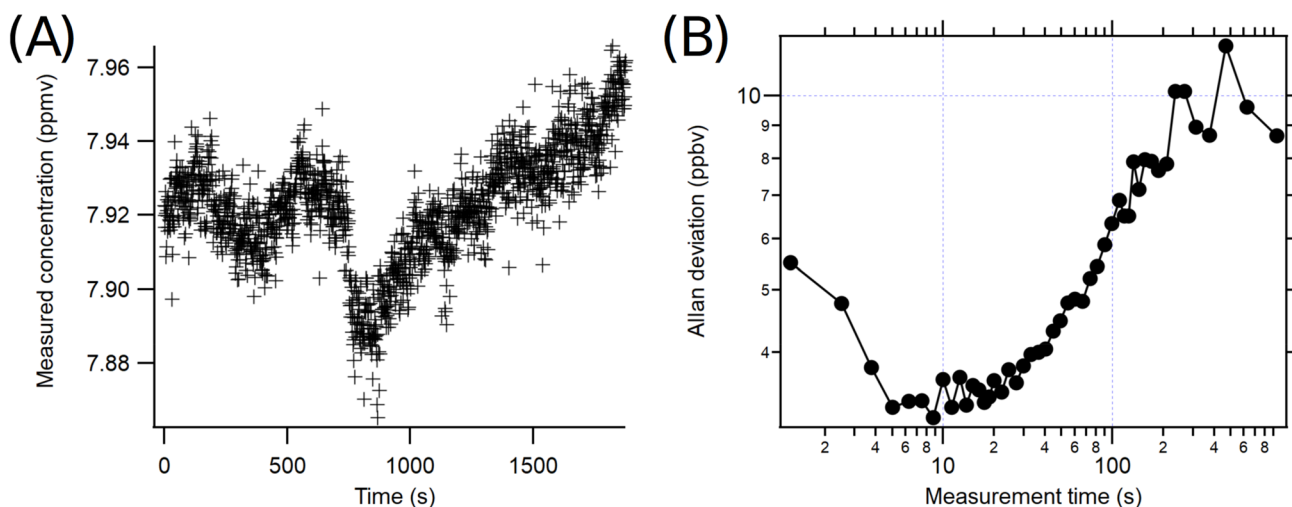


Fig. 4 **a** Measured concentrations of an ~8 ppmv isoprene mixture over a period of 30 min using the QCL spectrometer. **b** Allan deviation plot based on the data in (a). The minimum value of the Allan deviation is found at an averaging time of 9 s, with a value of 3.2 ppbv

placing sorbothane underneath the cell, but still notice that the signal on the detector is affected by vibrations in the laser table (i.e., when tapping the optical table, a ripple can be seen in the detector signal).

4 Isoprene measurements in human breath

Concentrations of isoprene in human breath vary considerably, but previous studies performed using mass spectrometry give a sense of the expected range of values. The isoprene concentration is quite variable, but an analysis of healthy volunteers has shown an average concentration of isoprene in breath of 120 ppbv with a standard deviation of 70 ppbv [33]. Using this approximate value, our current instrument is capable of measuring isoprene in breath samples, but there are some complications due to interfering species.

Some of the main interfering species in this region of the infrared spectrum are ammonia, methanol, and carbon dioxide. Figure 5 shows simulated absorption spectra for a typical breath sample prepared using the SpectraPlot website [32] for ammonia, methanol, and carbon dioxide, as well as simulated isoprene spectra based on our measurements. We have included simulations at atmospheric pressure and at reduced pressure (190 Torr) to show the effect of pressure broadening. As seen in the figure, there are strong ammonia and carbon dioxide peaks to the red of the main isoprene Q-branch peak we are using for our concentration measurements. In addition, there are many weak methanol features throughout this frequency region. Both ammonia

and methanol occur naturally in human breath at higher concentrations than isoprene, at typical concentrations of several hundred ppbv. Carbon dioxide is present at very high concentrations in exhaled breath, on the order of several percent. At atmospheric pressure, the wings of the pressure-broadened ammonia and carbon dioxide lines interfere with the isoprene peak we have observed. At reduced pressure, the isoprene peak can be resolved because of the reduced linewidths of the interfering species, though both the isoprene, ammonia, and carbon dioxide peaks will need to be fit simultaneously when determining concentrations. Absorption peaks due to water vapor are very weak in this region of the spectrum, and have negligible absorbance in comparison to ammonia, methanol, and carbon dioxide even at the high water vapor concentrations found in human breath. This is one of the main advantages of using this spectral region for our measurements.

As can be seen above, it is preferable to measure our spectra at lower pressure to reduce overlap with interfering species. Unfortunately, because the isoprene peak we are observing is due to a Q-branch composed of many overlapping peaks, the absorption peak significantly decreases in intensity as the pressure broadening decreases. This leads to a decreased signal-to-noise ratio for our spectra at reduced pressure. Figure 6 shows spectra of the standard 10.5 ppmv isoprene sample measured at several pressures, showing the decreased signal as the pressure decreases. We have characterized our spectrometer at a lower pressure of 190 Torr and have still seen linear concentration behavior, though the lowest noise-equivalent concentration of the instrument

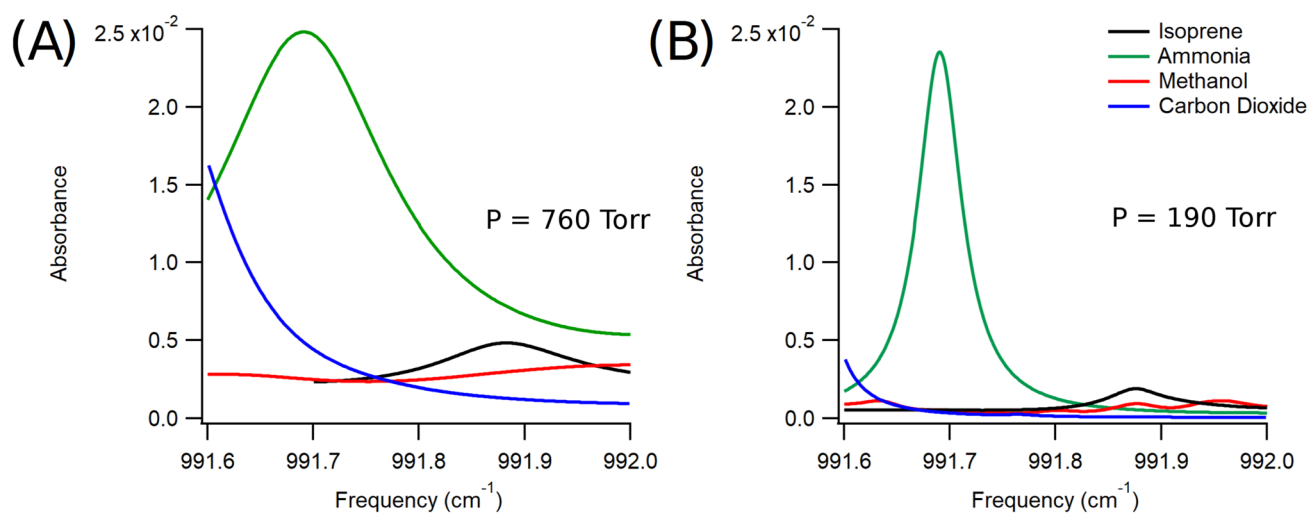
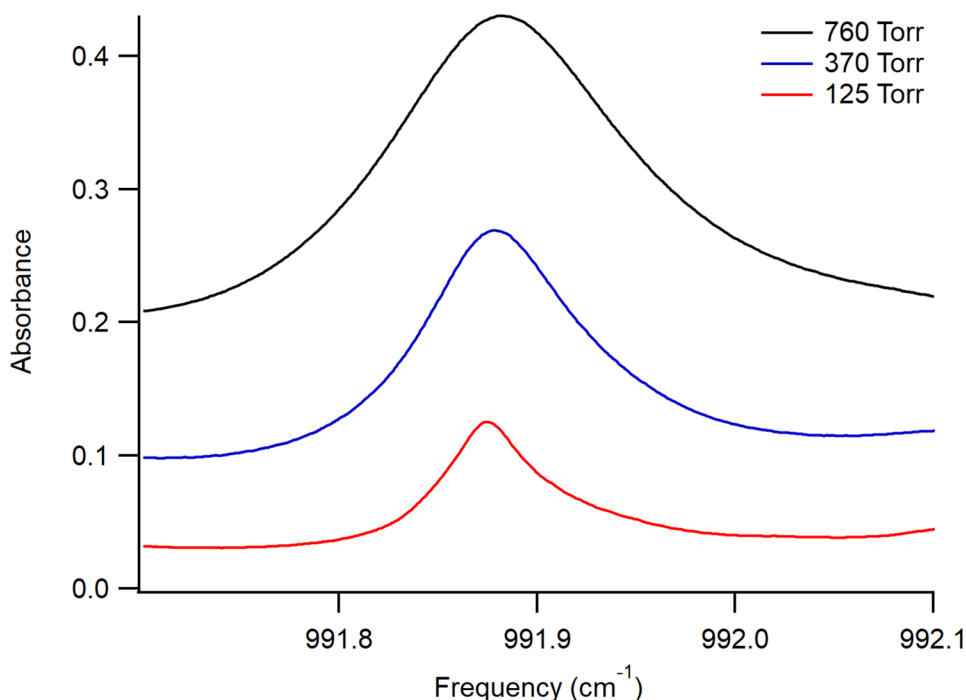


Fig. 5 Simulated spectra of isoprene (black), ammonia (green), methanol (red), and carbon dioxide (blue) in the range of the isoprene Q-branch used for determining isoprene concentrations. **a** Shows a simulation at a pressure of 760 Torr and **b** shows a simulation at a pressure of 190 Torr. The isoprene simulations are based on our measurements and the ammonia, methanol, and carbon dioxide simu-

lations were made using SpectraPlot [32]. All simulations are made for a sample measured in our multipass cell with a 76 m pathlength at a temperature of 300 K, with assumed concentrations of 120 ppbv for isoprene, 830 ppbv for ammonia, 460 ppbv for methanol, and 4% for carbon dioxide

Fig. 6 Isoprene absorbance peak as a function of pressure. The three absorbance spectra of the 10.5 ppmv isoprene sample were acquired at pressures of 760 Torr (black, top), 370 Torr (blue, middle), and 125 Torr (red, bottom)



increases to 9 ppbv because of the decreased signal at lower pressures (see Figs. 7 and 8).

To demonstrate the capabilities of our spectrometer with a real-world sample, we collected breath samples from a healthy volunteer and measured them using the QCL-based spectrometer. The breath samples were collected by having the volunteer breathe directly into a Tedlar bag after a brief period (30 s) of light exercise. The samples were transferred to the multipass cell and measured using the spectrometer without any further processing. The breath samples were

kept at a pressure of 190 Torr during data acquisition and 10 spectra of the sample were obtained at an acquisition time of 0.25 s per spectrum, and then the 10 spectra were averaged. This same process was repeated for a background measurement of nitrogen at 190 Torr, which was used to obtain the absorption spectrum. The averaged absorption spectra of the breath samples are shown in Fig. 9. Three main absorption peaks can be seen in the spectrum: The peak at 991.56 cm⁻¹ is due to carbon dioxide, the peak at 991.69 cm⁻¹ is due to ammonia, and the peak at 991.87 cm⁻¹ is due to isoprene.

Fig. 7 Comparison of measured isoprene concentrations using the QCL spectrometer and the prepared concentrations made by diluting the certified isoprene sample. The measurements presented in this figure were made at a pressure of 190 Torr in the multipass cell. The instrument is still highly linear at reduced pressure with a slope of nearly 1 for the best-fit line

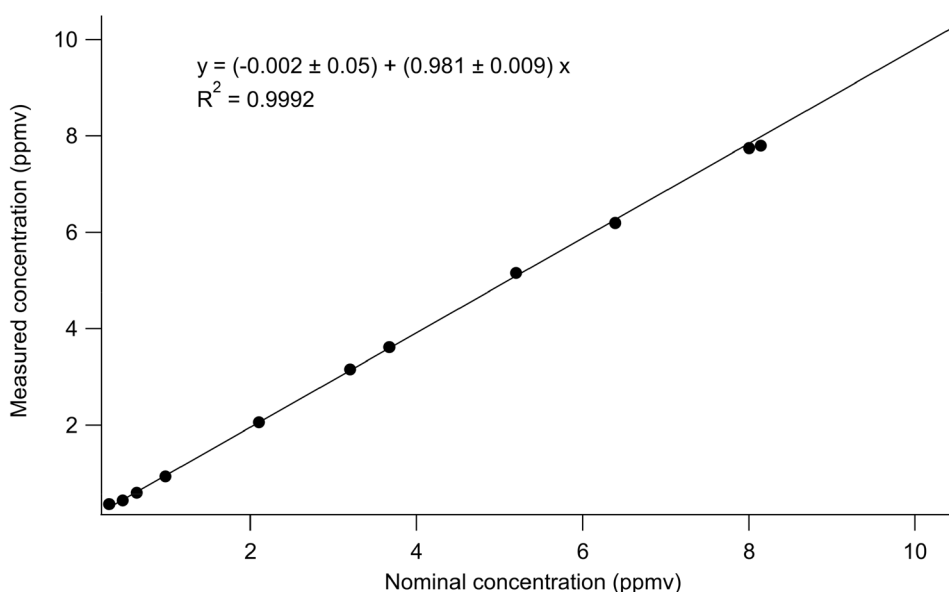
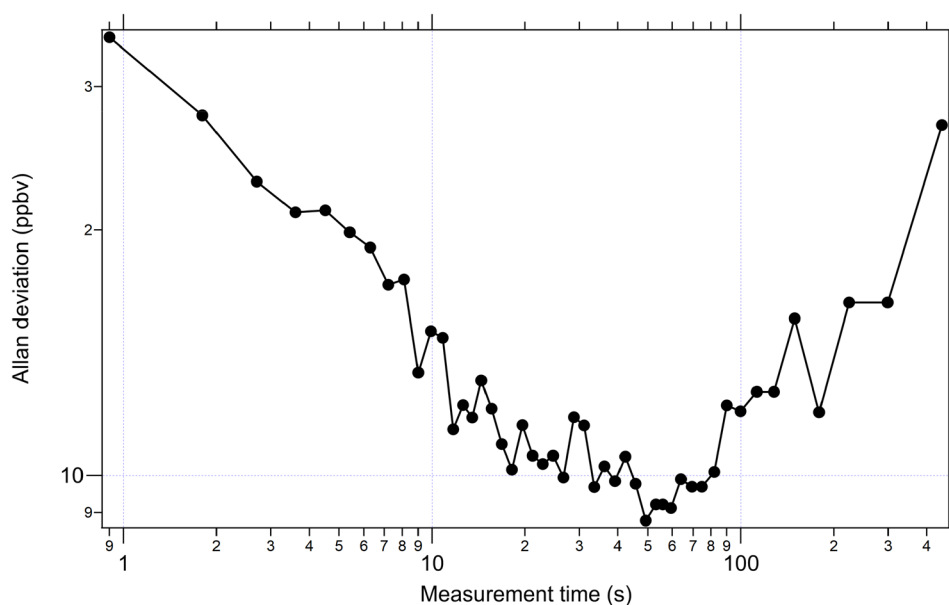


Fig. 8 Allan deviation plot for 15 min of isoprene measurements of the certified isoprene sample made using the QCL spectrometer at a reduced pressure of 190 Torr in the multipass cell. The lowest noise-equivalent concentration under these conditions is 9 ppbv at an optimal averaging time of 50 s



To retrieve concentrations from these spectra, we fit the isoprene, ammonia, and carbon dioxide peaks simultaneously using linear least squares fitting (a similar approach has been used previously [34]). The spectrum was fit to the following equation:

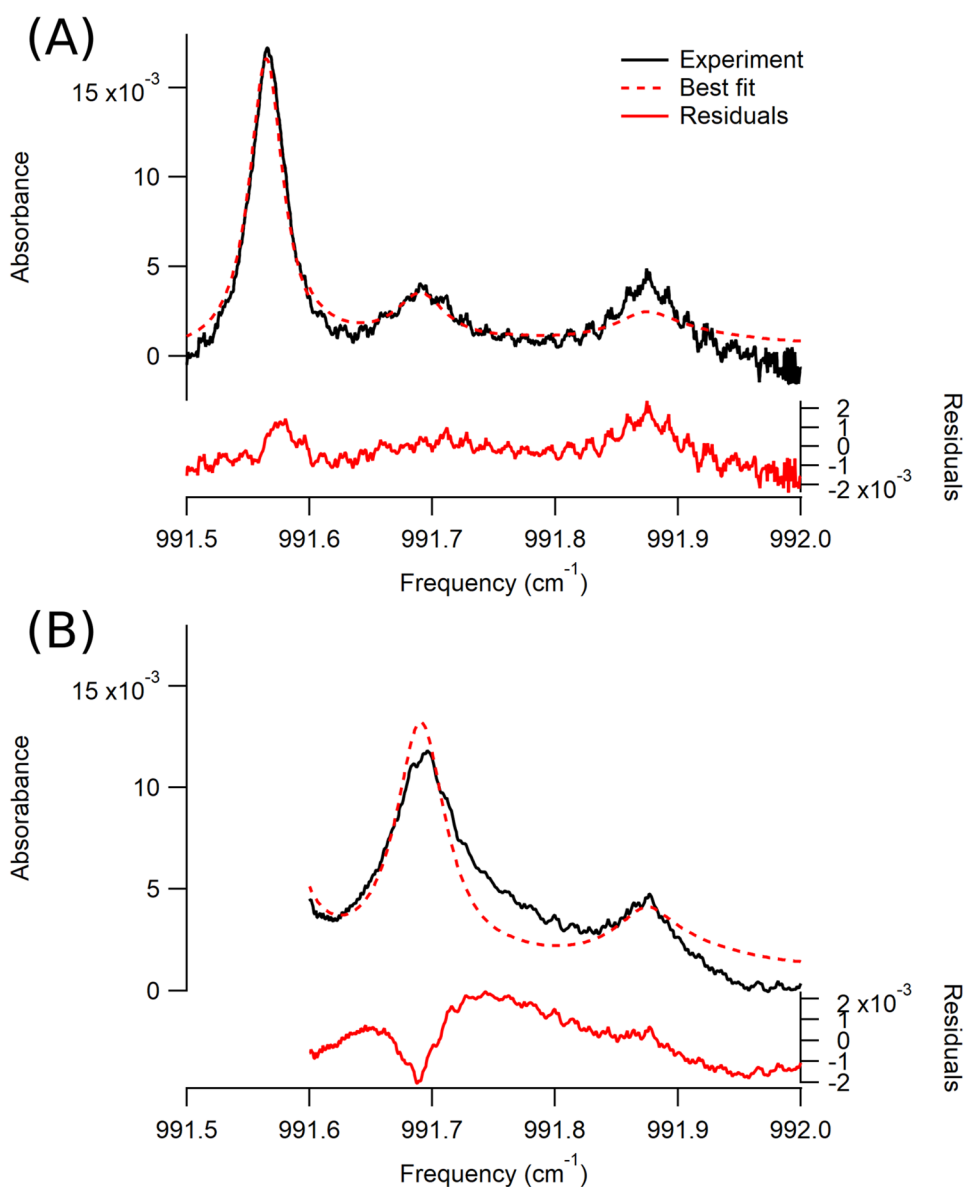
$$A_{\text{measured}}(\tilde{\nu}) = c_{\text{iso}} \times A_{\text{iso,ref}}(\tilde{\nu}) + c_{\text{amm}} \times A_{\text{amm,ref}}(\tilde{\nu}) + c_{\text{CO}_2} \times A_{\text{CO}_2,\text{ref}}(\tilde{\nu}) \quad (2)$$

Here, A_{measured} is the measured absorption spectrum, $A_{\text{iso,ref}}$ is a reference isoprene absorption spectrum, $A_{\text{amm,ref}}$ is a reference ammonia absorption spectrum, $A_{\text{CO}_2,\text{ref}}$ is a reference carbon dioxide absorption spectrum, c_{iso} is the isoprene concentration in ppmv, c_{amm} is the ammonia concentration in ppmv, and c_{CO_2} is the carbon dioxide concentration in percent. For the reference isoprene spectrum, we used a previously measured absorption spectrum of the certified isoprene mixture obtained at 190 Torr and scaled to the expected absorption for a 1 ppmv sample in our multipass cell. For the reference ammonia and carbon dioxide spectra, we used SpectraPlot to simulate the absorption spectrum of a 1 ppmv sample (for ammonia) or a 1% sample (for carbon dioxide) with a pathlength of 76 m at a pressure of 190 Torr and a temperature of 300 K. The concentrations given by the fit for the spectrum in Fig. 9a are: isoprene, 130 ± 20 ppbv; ammonia, 90 ± 10 ppbv; and carbon dioxide, $3.08 \pm 0.06\%$. The concentrations from the fit for the spectrum in Fig. 9b are: isoprene, 210 ± 20 ppbv; ammonia, 420 ± 20 ppbv; and carbon dioxide, $3.3 \pm 0.9\%$. The uncertainties given represent the 3σ standard errors from the least squares fit. The magnitude of the residuals of each fit (shown at the bottom of each spectrum in Fig. 9) is similar to the residuals we have

observed when fitting only isoprene (see the residuals at the bottom of Fig. 2). It is unclear why the ammonia concentration is so low for the breath sample shown in Fig. 9a. The retrieved value is significantly lower than typical ammonia concentrations measured for healthy individuals using mass spectrometry [35]. The other measured value for ammonia and the measured isoprene concentrations are within the ranges measured for healthy individuals using mass spectrometry [33, 35].

There are several possible ways to improve the instrument to enhance its performance. First, there are two vibrational bands of isoprene with even stronger intensities located at 894 and 906 cm^{-1} , which also have strong Q-branches that could be exploited for sensing applications. Based on previous measurements, these bands are roughly twice as strong as the ν_{26} band we used for this work [29]. The lower frequency bands can be accessed by commercial QCLs, but we do not currently have a laser that can reach these frequencies. A second prospect is using preconcentration to enhance the signal in the spectrometer. Preconcentration was successfully used by Perez-Guatia et al. to improve the limit of detection of their isoprene sensor by a factor of 120 [30]. The downside is that the improved sensitivity offered by preconcentration comes at the cost of increasing the complexity of the measurement and decreasing the temporal resolution of the spectrometer. Third, wavelength modulation spectroscopy is an additional way to decrease the noise in our measurement. We have attempted wavelength modulation spectroscopy with our current QCL system, but because the isoprene peak is quite broad, we are unable to achieve a sufficient modulation depth to obtain a useful improvement in our signal-to-noise ratio. Wavelength modulation

Fig. 9 Absorption spectra of two breath samples from a healthy volunteer (black lines) with best-fit spectra accounting for isoprene, ammonia, and carbon dioxide (dashed red lines). The pressure inside the multipass cell for both samples was 190 Torr. For (a), the concentrations retrieved from the fit are: isoprene, 130 ± 20 ppbv; ammonia, 90 ± 10 ppbv; and carbon dioxide, $3.08 \pm 0.06\%$. For (b), the concentrations retrieved from the fit are: isoprene, 210 ± 20 ppbv; ammonia, 420 ± 20 ppbv; and carbon dioxide, $3.3 \pm 0.9\%$. The uncertainties given are 3σ standard errors from the least squares fit. The residuals of the fit (solid red lines) are included at the bottom of each spectrum



spectroscopy of a broad spectral feature has been performed previously with a homemade EC-QCL [36], showing that this approach is possible for future isoprene measurements. Finally, the stability of the instrumental setup can be improved to reduce drift and allow for longer averaging times to reduce the detection limit. These potential improvements may allow a QCL-based spectrometer to be used for measuring isoprene in atmospheric samples, where the isoprene concentrations are significantly lower than in exhaled breath (in the range of 0–10 ppbv in forest environments [37] and lower (0–2 ppbv) in urban environments [6]).

5 Conclusion

We have used a QCL-based infrared spectrometer to perform sensitive measurements of isoprene down to the ppbv range of concentrations. The spectrometer exhibits linear behavior over the range of isoprene concentrations we have studied (0.3–10.5 ppmv) and the lowest noise-equivalent concentration measured for the instrument is 3.2 ppbv at an optimal averaging time of 9 s when measurements are performed at atmospheric pressure. The lowest noise-equivalent concentration increases to 9 ppbv when the measurements are done at a decreased pressure of 190 Torr. As a tradeoff, the decreased linewidths at lower pressures cause decreased interference from other common species in atmospheric and breath samples, namely ammonia, methanol,

and carbon dioxide. The current spectrometer is capable of measuring isoprene (and ammonia) concentrations in human breath samples, and we have measured breath samples from a healthy volunteer to demonstrate this capability, finding an isoprene concentrations of 130 ± 20 and 210 ± 20 ppbv. While the accuracy of this measurement has not been verified by a different technique, it is well within the range of previously measured isoprene concentrations for healthy individuals. We have also discussed prospects for improving the spectrometer, which may allow it to be used for measurements of atmospheric samples. QCL-based infrared spectroscopy is a promising method for obtaining rapid and reliable measurements of isoprene concentrations in atmospheric and breath applications.

Acknowledgements The authors thank Dave Lewis for the loan of the multipass cell that was used in the present work. This work was supported by startup funding from Connecticut College.

References

1. A. H. Steiner and A. L. Goldstein, in *Volatile Organic Compounds in the Atmosphere*, edited by R. Koppmann (Blackwell Publishing Ltd, Oxford, 2007), pp. 83–127.
2. A.B. Guenther, X. Jiang, C.L. Heald, T. Sakulyanontvittaya, T. Duhl, L.K. Emmons, X. Wang, *Geosci. Model Dev.* **5**, 1471–1492 (2012)
3. M. Claeys, B. Graham, G. Vas, W. Wang, R. Vermeylen, V. Pashynska, J. Cafmeyer, P. Guyon, M.O. Andreae, P. Artaxo, W. Maenhaut, *Science* **303**, 1173–1176 (2004)
4. D.R. Worton, J.D. Surratt, B.W. LaFranchi, A.W.H. Chan, Y. Zhao, R.J. Weber, J.-H. Park, J.B. Gilman, J. de Gouw, C. Park, G. Schade, M. Beaver, J.M. St. Clair, J. Crouse, P. Wennberg, G.M. Wolfe, S. Harrold, J.A. Thornton, D.K. Farmer, K.S. Docherty, M.J. Cubison, J.-L. Jimenez, A.A. Frossard, L.M. Russell, K. Kristensen, M. Glasius, J. Mao, X. Ren, W. Brune, E.C. Browne, S.E. Pusede, R.C. Cohen, J.H. Seinfeld, A.H. Goldstein, *Environ. Sci. Technol.* **47**, 11403–11413 (2013)
5. R. Atkinson, J. Arey, *Atmos. Environ.* **37**, 197–219 (2003)
6. Z. Mo, M. Shao, W. Wang, Y. Liu, M. Wang, S. Lu, *Sci. Total Environ.* **627**, 1485–1494 (2018)
7. R. Salerno-Kennedy, K.D. Cashman, *Wien. Klin. Wochenschr.* **117**, 180–186 (2005)
8. N. Alkhoury, T. Singh, E. Alsabbagh, J. Guirguis, T. Chami, I. Hanouneh, D. Grove, R. Lopez, R. Dweik, *Clin. Transl. Gastroenterol.* **6**, e112–e117 (2015)
9. C. Stöner, A. Edtbauer, B. Derstroff, E. Bourtsoukidis, T. Klüpfel, J. Wicker, J. Williams, *PLoS ONE* **13**, 1–14 (2018)
10. J.A. de Gouw, P.D. Goldan, C. Warneke, W.C. Kuster, J.M. Roberts, M. Marchewka, S.B. Bertman, A.A.P. Pszenny, W.C. Keene, *J. Geophys. Res. Atmos.* **108**, 1–18 (2003)
11. J. De Gouw, C. Warneke, *Mass Spectrom. Rev.* **26**, 223–257 (2007)
12. A.T. Güntner, N.J. Pineau, D. Chie, F. Krumeich, S.E. Pratsinis, *J. Mater. Chem. B* **4**, 5358–5366 (2016)
13. J. Van Den Broek, A.T. Güntner, S.E. Pratsinis, *ACS Sens.* **3**, 677–683 (2018)
14. Y. Park, R. Yoo, S. Ryull Park, J.H. Lee, H. Jung, H.S. Lee, W. Lee, *Sens. Actuators B Chem.* **290**, 258–266 (2019)
15. J. Rinne, T. Karl, A. Guenther, *Atmos. Environ.* **131**, 225–227 (2016)
16. L.S. Rothman, I.E. Gordon, Y. Babikov, A. Barbe, D. Chris Benner, P.F. Bernath, M. Birk, L. Bizzocchi, V. Boudon, L.R. Brown, A. Campargue, K. Chance, E.A. Cohen, L.H. Coudert, V.M. Devi, B.J. Drouin, A. Fayt, J.M. Flaud, R.R. Gamache, J.J. Harrison, J.M. Hartmann, C. Hill, J.T. Hodges, D. Jacquemart, A. Jolly, J. Lamouroux, R.J. Le Roy, G. Li, D.A. Long, O.M. Lyulin, C.J. Mackie, S.T. Massie, S. Mikhailenko, H.S.P. Müller, O.V. Naumenko, A.V. Nikitin, J. Orphal, V. Perevalov, A. Perrin, E.R. Polovtseva, C. Richard, M.A.H. Smith, E. Starikova, K. Sung, S. Tashkun, J. Tennyson, G.C. Toon, V.G. Tyuterev, G. Wagner, *J. Quant. Spectrosc. Radiat. Transf.* **130**, 4–50 (2013)
17. S.W. Sharpe, T.J. Johnson, R.L. Sams, P.M. Chu, G.C. Rhoderick, P.A. Johnson, *Appl. Spectrosc.* **58**, 1452–1461 (2004)
18. J.S. Li, W. Chen, H. Fischer, *Appl. Spectrosc. Rev.* **48**, 523–559 (2013)
19. J. Sun, J. Ding, N. Liu, G. Yang, J. Li, *Spectrochim. Acta Part A Mol. Biomol. Spectrosc.* **191**, 532–538 (2018)
20. Z. Du, S. Zhang, J. Li, N. Gao, K. Tong, *Appl. Sci.* **9**, 338 (2019)
21. D.J. Miller, K. Sun, L. Tao, M.A. Khan, M.A. Zondlo, *Atmos Meas. Tech.* **7**, 81–93 (2014)
22. I. B. Pollack, J. Lindaas, J. R. Roscioli, M. Agnese, W. Permar, L. Hu, and E. V. Fischer, *Atmos. Meas. Tech. Discuss.* 1–36 (2019).
23. N.S. Daghestani, R. Brownsword, D. Weidmann, *Opt. Express* **22**, A1731 (2014)
24. Y. Cao, N.P. Sanchez, W. Jiang, R.J. Griffin, F. Xie, L.C. Hughes, C. Zah, F.K. Tittel, *Opt. Express* **23**, 2121 (2015)
25. J. Li, H. Deng, J. Sun, B. Yu, H. Fischer, *Sens. Actuators B Chem.* **231**, 723–732 (2016)
26. O. Aseev, B. Tuzson, H. Looser, P. Scheidegger, C. Liu, C. Morstein, B. Niederhauser, L. Emmenegger, *Opt. Express* **27**, 5314–5325 (2019)
27. F. Kühnemann, M. Wolfertz, S. Arnold, M. Lagemann, A. Popp, G. Schüler, A. Jux, W. Boland, *Appl. Phys. B Lasers Opt.* **75**, 397–403 (2002)
28. F. Adler, P. Masłowski, A. Foltynowicz, K.C. Cossel, T.C. Briles, I. Hartl, J. Ye, *Opt. Express* **18**, 21861–21872 (2010)
29. C.S. Brauer, T.A. Blake, A.B. Guenther, S.W. Sharpe, R.L. Sams, T.J. Johnson, *Atmos Meas. Tech.* **7**, 3839–3847 (2014)
30. D. Perez-Guaita, V. Kokoric, A. Wilk, S. Garrigues, B. Mizaikoff, *J. Breath Res.* **8**, 26003 (2014)
31. M.V. Pinto Pereira, T.P. Hoadley, M.C. Iranpour, M.N. Tran, J.T. Stewart, *J. Mol. Spectrosc.* **350**, 37–42 (2018)
32. C.S. Goldenstein, V.A. Miller, R. Mitchell Spearrin, C.L. Strand, *J. Quant. Spectrosc. Radiat. Transf.* **200**, 249–257 (2017)
33. C. Turner, P. Španěl, D. Smith, *Physiol. Meas.* **27**, 13–22 (2006)
34. S. Zhou, Y. Han, B. Li, *Appl. Phys. B Lasers Opt.* **122**, 1–8 (2016)
35. C. Turner, P. Španěl, D. Smith, *Physiol. Meas.* **27**, 321–337 (2006)
36. F. Nadeem, J. Mandon, A. Khodabakhsh, S. Cristescu, F. Harren, *Sensors* **18**, 2050 (2018)
37. C. Kalogridis, V. Gros, R. Sarda-Estève, B. Langford, B. Loubet, B. Bonsang, N. Bonnaire, E. Nemitz, A.C. Genard, C. Boissard, C. Fernandez, E. Ormeño, D. Baisnée, I. Reiter, J. Lathière, *Atmos. Chem. Phys.* **14**, 10085–10102 (2014)

Publisher's Note Springer Nature remains neutral with regard to jurisdictional claims in published maps and institutional affiliations.